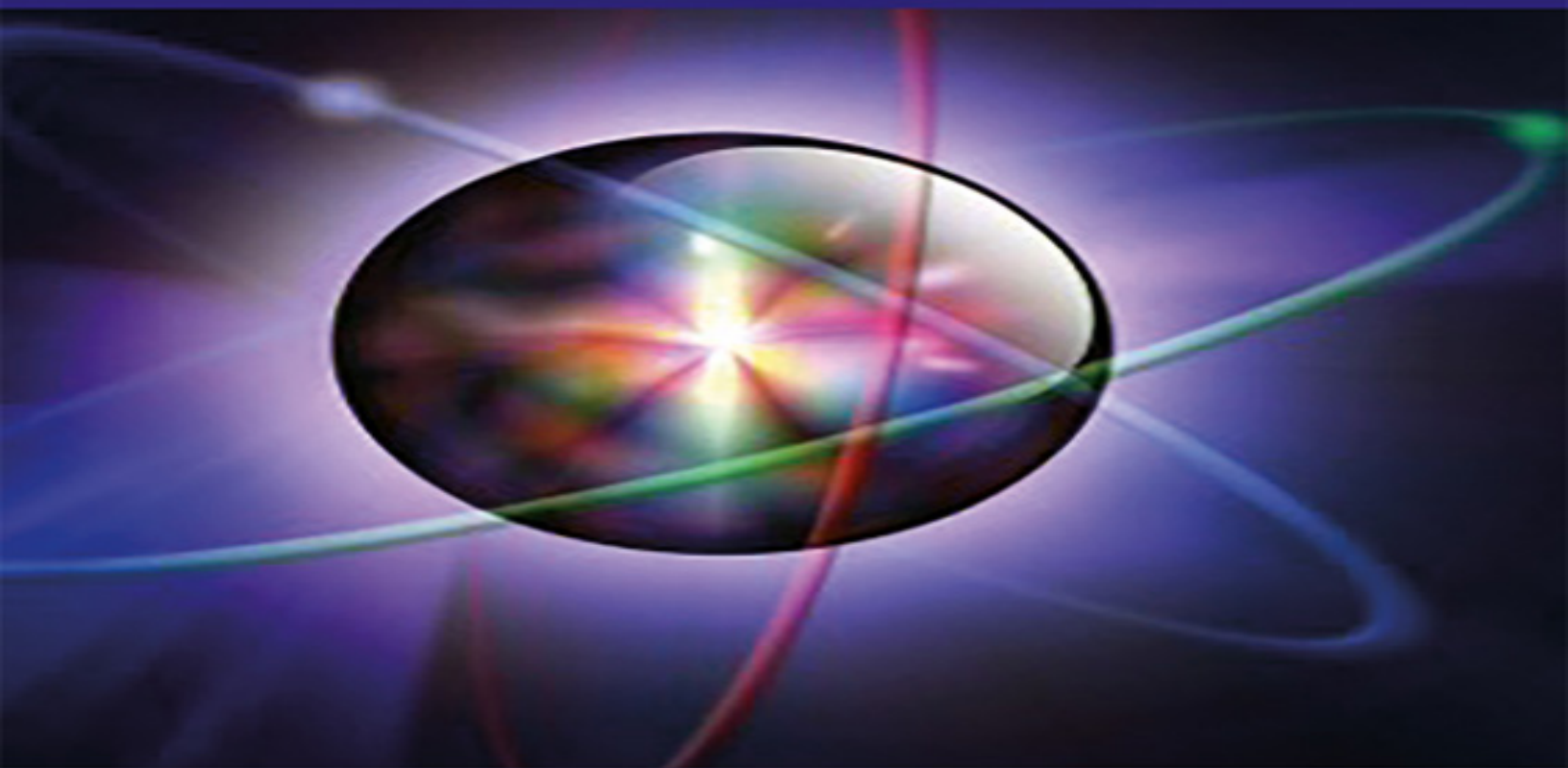


WAVES SERIES

Nuclear Physics 1

*Nuclear Deexcitations, Spontaneous
Nuclear Reactions*

Ibrahima Sakho



ISTE

WILEY

Table of Contents

[Cover](#)

[Title Page](#)

[Copyright](#)

[Preface](#)

[1 Overview of the Nucleus](#)

[1.1. Discovery of the electron](#)

[1.2. The birth of the nucleus](#)

[1.3. Composition of the nucleus](#)

[1.4. Nucleus dimensions](#)

[1.5. Nomenclature of nuclides](#)

[1.6. Nucleus stability](#)

[1.7. Exercises](#)

[1.8. Solutions to exercises](#)

[2 Nuclear Deexcitations](#)

[2.1. Nuclear shell model](#)

[2.2. Angular momentum and parity](#)

[2.3. Gamma deexcitation](#)

[2.4. Internal conversion](#)

[2.5. Deexcitation by nucleon emission](#)

[2.6. Bethe-Weizsäcker semi-empirical mass formula](#)

[2.7. Mass parabola equation for odd \$A\$](#)

[2.8. Nuclear potential barrier](#)

[2.9. Exercises](#)

[2.10. Solutions to exercises](#)

[3 Alpha Radioactivity](#)

[3.1. Experimental facts](#)

[3.2. Radioactive decay](#)

[3.3. \$\alpha\$ radioactivity](#)

[3.4. Exercises](#)

[3.5. Solutions to exercises](#)

[4 Beta Radioactivity, Radioactive Family Tree](#)

[4.1. Beta radioactivity](#)

[4.2. Radioactive family trees](#)

[4.3. Radionuclide production by nuclear bombardment](#)

[4.4. Natural radioactive series](#)

[4.5. Exercises](#)

[4.6. Solutions to exercises](#)

[Appendices](#)

[Appendix 1 Quantified Energy of the Three-Dimensional Quantum Harmonic Oscillator](#)

[A1.1. Integration of the Schrödinger equation](#)

[A1.2. Use of creation and annihilation operators](#)

[Appendix 2 Atomic Masses of Several Nuclides](#)

[References](#)

[Index](#)

[End User License Agreement](#)

List of Illustrations

Chapter 1

[Figure 1.1. Crookes tube](#)

[Figure 1.2. Crookes tube wall fluorescence](#)

[Figure 1.3. Perrin's simplified experimental set-up](#)

[Figure 1.4. Simplified set-up for measuring the electron mass-to-charge ratio: \(...\)](#)

[Figure 1.5a. *Millikan's simplified experimental device*](#)

[Figure 1.5b. Uniform drop motion of a droplet of charge \$q\$, mass \$m\$ and radius \$r\$](#)

[Figure 1.6. *Planetary model of the atom, envisioned by Perrin in 1901*](#)

[Figure 1.7. *Model of the atom envisioned by Thomson*](#)

[Figure 1.8. *Simplified experimental device by Geiger and Marsden*](#)

[Figure 1.9. *Rutherford scattering experiment set-up*](#)

[Figure 1.10. *Planetary atomic model envisaged by Rutherford*](#)

[Figure 1.11. *Scattering of a beam of \$\alpha\$ particles of an angle, \$\theta\$, in the solid ang...*](#)

[Figure 1.12. *Frontal collision between an \$\alpha\$ particle and an immobile nucleus of ...*](#)

[Figure 1.13. *Comparisons of theoretical predictions according to the Rutherford ...*](#)

[Figure 1.14. *Rutherford's simplified experimental device for conducting the firs...*](#)

[Figure 1.15. *Chadwick's experimental set-up*](#)

[Figure 1.16. *Internal proton and neutron structures according to the Gell-Mann a...*](#)

[Figure 1.17. *Variation of the nuclear charge distribution density \$\rho\$ \(r\); the nuc...*](#)

[Figure 1.18. Segrè diagram, the nuclear energy surface indicated in red, groupin...](#)

[Figure 1.19. Energy \$E_I\$ necessary to separate, to infinity, the nucleons of a nuc...](#)

[Figure 1.20. *Aston curve*](#)

[Figure 1.21. Comparison of the stability of the nuclei of uranium-238, strontium...](#)

[Figure 1.22. Simplified Thomson device for identifying the canal rays discovered...](#)

[Figure 1.23. *Simplified diagram of a mass spectrograph*](#)

[Figure 1.24. *Uranium isotope trajectories in a magnetic deflector*](#)

[Figure 1.25. Portion of the trajectory of a particle of charge \$q\$ in motion in a ...](#)

[Figure 1.26. *Circular trajectories of isotope ions in the magnetic deflector*](#)

Chapter 2

[Figure 2.1. *Profile of a harmonic potential well of depth \$V_0\$*](#)

[Figure 2.2. Nucleon distribution according to the shell model for helium-4 and l...](#)

[Figure 2.3. Nucleon distribution according to the shell model for the neon-18 nu...](#)

[Figure 2.4. *Shape of the Woods-Saxon potential*](#)

[Figure 2.5. Shape of the Woods-Saxon potential for nuclei of mass number 16, 40,...](#)

[Figure 2.6. Comparison of shell structures derived from a harmonic potential and...](#)

[Figure 2.7. Comparison of shell structures derived from a harmonic potential and...](#)

[Figure 2.8. Ground state of the helium-4 nucleus, \$J^\pi = 0^+\$; \(a\) distribution deri...](#)

[Figure 2.9. Ground state of the lithium-6 nucleus, \$J^\pi = 1+\$; and three excited st...](#)

[Figure 2.10. Ground state of the nucleus of lithium-6, \$J^\pi = 3/2^-\$; and the first ...](#)

[Figure 2.11. Ground state, \$J^\pi = 0^+\$; and excited states \(\$J^\pi = 2^+\$, \$J^\pi = 4+\$ \) of the...](#)

[Figure 2.12. Ground state of the magnesium-25 nucleus, \$J^\pi = 5/2+\$; and the two ex...](#)

[Figure 2.13. \$\gamma\$ -transitions to the ground level of the nickel-60 nucleus](#)

[Figure 2.14. \$\gamma\$ -transitions to the ground level of the barium-137 nucleus](#)

[Figure 2.15. Competition of \$\gamma\$ -deexcitation and the internal conversion process](#)

[Figure 2.16. Electric monopole transition, \$E0\$, resulting from a process of initi...](#)

[Figure 2.17. Variation in the internal conversion coefficient, \$\alpha_K\$ with atomic nu...](#)

[Figure 2.18. Variation in internal conversion coefficients \(\$\alpha_K\$ \)_{el} and \(\$\alpha_K\$ \)_{mag} re...](#)

[Figure 2.19. General diagram of nuclear deexcitation by delayed-neutron emission...](#)

[Figure 2.20. Bound levels and virtual levels of the nitrogen-14 nucleus. All lev...](#)

[Figure 2.21. Diagram of nuclear deexcitation by delayed-neutron emission by the ...](#)

[Figure 2.22. Summary of the treatment of binding energy within the framework of ...](#)

[Figure 2.23. *Mass parabola for the isobars of odd A*](#)

[Figure 2.24. Mass parabola for the isobars of even A. Note that there are two pa...](#)

[Figure 2.25. Profile of the nuclear potential barrier between a nucleus of charg...](#)

[Figure 2.26. Modified profile of the nuclear potential barrier between a nucleus...](#)

[Figure 2.27. *Nuclear levels of platinum-188 and thorium-228.* For clarity, the en...](#)

[Figure 2.28. *\$\gamma\$ -transitions to the ground level of the neon-22 nucleus*](#)

[Figure 2.29. Curve indicating the variation in the Napierian logarithm of the ra...](#)

[Figure 2.30a. Shell structure derived from a harmonic potential \(a\) and distribu...](#)

[Figure 2.30b. Shell structure derived from a harmonic potential \(a\) and distribu...](#)

[Figure 2.30c. Shell structure derived from a harmonic potential \(a\) and distribu...](#)

[Figure 2.31. *Charge \$Q\(r\)\$ contained in the nuclear envelope with radius \$r\$*](#)

[Figure 2.32. Internal and external electric fields created by charges \$Q\(r\)\$ and ...](#)

Chapter 3

[Figure 3.1. Creation of electron-positron pair by a process of materialization o...](#)

[Figure 3.2. Process of annihilation of an electron-positron pair with production...](#)

[Figure 3.3. Neutron decay by low interaction. It is the decay of the \$W^-\$ boson in...](#)

[Figure 3.4. Proton decay by low interaction. It is the decay of the \$W^+\$ boson int...](#)

[Figure 3.5. Cowan and Reines experimental set-up](#)

[Figure 3.6. Separation, by a uniform electric field, of \$\alpha\$, \$\beta\$ and \$\gamma\$ radiations em...](#)

[Figure 3.7. Exponential decay of the number, \$N\(t\)\$, of radioactive nuclei](#)

[Figure 3.8. \$\alpha\$ decay energy diagram](#)

[Figure 3.9. Uranium-232 \$\alpha\$ decay energy diagram](#)

[Figure 3.10. Variation of curve \$\ln T = f\(E_\alpha^{1/2}\)\$ for several \$\alpha_Z X\$ emitters \(polonium \$_{84}\text{Po}\$, prota...](#)

[Figure 3.11. Modeling of \$\alpha\$ emission by tunnel effect. The barrier width is equal...](#)

[Figure 3.12. Curve of variation as a function of time of the opposite of the Nap...](#)

[Figure 3.13. Uranium-233 \$\alpha\$ decay energy diagram](#)

Chapter 4

[Figure 4.1a. Experimental set-up of Frédéric and Irène Joliot-Curie that led to ...](#)

[Figure 4.1b. Experimental set-up of Frédéric and Irène Joliot-Curie that led to ...](#)

[Figure 4.2a. Description of a Geiger-Müller counter](#)

[Figure 4.2b. Measuring principle using a Geiger-Müller counter. Source: https://...](#)

[Figure 4.3. \$\beta^-\$ emission spectrum of phosphorus-32](#)

[Figure 4.4. \$\beta^\pm\$ emission spectrum of phosphorus-30](#)

[Figure 4.5. Sargent diagram in its original form according to \[SAR 33\]](#)

[Figure 4.6. \$\beta^-\$ decay energy diagram of cesium-137 \(T = 32 years\). The diagram sh...](#)

[Figure 4.7. \$\beta^\pm\$ decay energy diagram of sodium-22 \(T = 2.58 years\). The diagram s...](#)

[Figure 4.8. Decay energy diagram of sodium-22 by electron capture \(EC\) and by \$\beta^\pm\$...](#)

[Figure 4.9. \$\alpha\$ and \$\beta^-\$ decay modes of radon-221](#)

[Figure 4.10. Process of atomic deexcitation by emission of X-rays or of an Auger...](#)

[Figure 4.11. Relative arrangement of the K-, L- and M-shells of copper atoms](#)

[Figure 4.12. Electron-hole recombination processes](#)

[Figure 4.13. Evolution curves of the activities of tellurium-131 and its daughte...](#)

[Figure 4.14. Variation in the activity, \$A_2\(t\)\$, of a radionuclide, \$X_2\$, obtained ...](#)

[Figure 4.15. Natural series of thorium. The stable end product of the family tre...](#)

[Figure 4.16. Artificial series of neptunium. The stable end product of the famil...](#)

[Figure 4.17. Natural series of uranium-235. The stable end product of the family...](#)

[Figure 4.18. Natural series of uranium-238 \(often called uranium-radium series\)....](#)

[Figure 4.19. Decay energy diagram of vanadium-48](#)

[Figure 4.20. Energy spectra of \$\beta\$ particles emitted by copper-64](#)

[Figure 4.21. \$\beta\$ decay energy diagram of indium-114](#)

[Figure 4.22. Distribution of nucleons of titanium-48: \(a\) shell structure derive...](#)

[Figure 4.23. Distribution of nucleons of vanadium-48: \(a\) shell structure derive...](#)

[Figure 4.24. The most probable electric quadrupole transitions \(E2\) between exci...](#)

[Figure 4.25. Decay energy diagram of vanadium-74](#)

[Figure 4.26. Maximum energy of \$\beta^-\$ and \$\beta^+\$ spectra of copper-64](#)

[Figure 4.27. Decay energy diagram of potassium-48. Of particular note are its th...](#)

List of Tables

Chapter 1

[Table 1.1. Fundamental properties of nucleons](#)

[Table 1.2. Molar percentages of the most significant isotopes of the first ten e...](#)

[Table 1.3. Electron and nucleon masses in \$u\$ and \$MeV/c^2\$](#)

Chapter 2

[Table 2.1. Order of the quantum states of a nucleon within the framework of the ...](#)

[Table 2.2. Properties of a nucleon subjected to a harmonic potential](#)

[Table 2.3. Classification of the \$\gamma\$ -transitions according to the multipole order](#)

[Table 2.4. Values of the \$C_{\ell}\(E\)\$ and \$C'_{\ell}\(E\)\$ coefficients for \$\gamma\$ -transitions](#)

[Table 2.5. Number of stable nuclei with respect to the parity of Z and N](#)

[Table 2.6. Calculating the average value of the ratio \$a_a/a_c\$](#)

[Table 2.7. Binding energy and atomic mass of some nuclides. The calculated value...](#)

[Table 2.8. Families of coefficients \$a_v, a_s, a_a, a_c\$ and \$a_p\$](#)

[Table 2.9. Values of Zmin calculated from the values of \$a_c\$ and \$a_a\$ gathered in Ta...](#)

[Table 2.10. Decay number \$\langle N \rangle\$ measured during a constant duration of 5s](#)

[Table 2.11. Comparison of the experimental \(\$B_{exp}\$ \) and theoretical \(\$B_{theo}\$ \) values...](#)

[Table 2.12. Theoretical values of the Coulomb coefficient and of the difference ...](#)

[Table 2.13. Comparison of the experimental \[MAR 69\] and theoretical values of th...](#)

[Table 2.14. Comparison of the experimental \[MAR 69\] and theoretical values of th...](#)

[Table 2.15. Values of the ratio \$A_0/A\(t\)\$ of the initial and instantaneous activit...](#)

[Table 2.16. Comparison of the experimental \(\$B_{exp}\$ \) and theoretical \(\$B_{theo}\$ \) values...](#)

[Table 2.17. Theoretical values of the Coulomb coefficient and of the difference ...](#)

[Table 2.18. Comparison of the experimental \[MAR 69\] and theoretical values of th...](#)

[Table 2.19. Comparison of the experimental \[MAR 69\] and theoretical values of th...](#)

Chapter 3

[Table 3.1. *Radioactive half-life of several radionuclides*](#)

[Table 3.2. *Energies of the \$\gamma\$ photons and \$\alpha\$ particles emitted during the decay of...*](#)

[Table 3.3. *Correlation between the radioactive half-life, \$T\$, and kinetic energy,...*](#)

[Table 3.4. *Variation as a function of time in the ratio of the number, \$N\(t\)\$, of ...*](#)

[Table 3.5. *Atomic masses of several nuclides*](#)

[Table 3.6. *Variation as a function of time of the opposite of the Napierian loga...*](#)

Chapter 4

[Table 4.1. *Several \(\$\beta, \gamma\$ \) emitters. The \(\$\beta^{\pm}, \gamma\$ \) emitters are all artificial*](#)

[Table 4.2. *Correspondence between the Siegbahn notation and that of the IUPAC in...*](#)

[Table 4.3. *Classification of energy levels and X-rays in Siegbahn notation*](#)

[Table 4.4. *Correspondence between old and conventional nucleus notations. The ra...*](#)

[Table 4.5. Correspondence between old and conventional nucleus notations. The ra...](#)

[Table 4.6. Correspondence between old and conventional nucleus notations. The ra...](#)

[Table 4.7. *Experimental values of maximum energy \$E_{max}\$ of the \$\beta^\pm\$ spectra of sever...*](#)

[Table 4.8. *Comparison of the experimental values of maximum energy, \$E_{max}\$, of the...*](#)

Appendix 2

[Table A2.1. *Atomic masses of nuclides with atomic numbers \$Z = 1-14\$*](#)

[Table A2.2. *Atomic masses of nuclides with atomic numbers \$Z = 14-38\$*](#)

[Table A2.3. *Atomic masses of nuclides with atomic numbers \$Z = 38-64\$*](#)

[Table A2.4. *Atomic masses of nuclides with atomic numbers \$Z = 65-93\$*](#)

Nuclear Physics 1

Nuclear Deexcitations, Spontaneous Nuclear Reactions

Ibrahima Sakho

ISTE

WILEY

First published 2021 in Great Britain and the United States by ISTE Ltd and John Wiley & Sons, Inc.

Apart from any fair dealing for the purposes of research or private study, or criticism or review, as permitted under the Copyright, Designs and Patents Act 1988, this publication may only be reproduced, stored or transmitted, in any form or by any means, with the prior permission in writing of the publishers, or in the case of reprographic reproduction in accordance with the terms and licenses issued by the CLA. Enquiries concerning reproduction outside these terms should be sent to the publishers at the undermentioned address:

ISTE Ltd
27-37 St George's Road
London SW19 4EU
UK

www.iste.co.uk

John Wiley & Sons, Inc.
111 River Street
Hoboken, NJ 07030
USA

www.wiley.com

© ISTE Ltd 2021

The rights of Ibrahima Sakho to be identified as the author of this work have been asserted by him in accordance with the Copyright, Designs and Patents Act 1988.

Library of Congress Control Number: 2021945496

British Library Cataloguing-in-Publication Data
A CIP record for this book is available from the British Library
ISBN 978-1-78630-641-8

Preface

Nuclear physics is devoted to the study of the properties of atomic nuclei. These properties relate to the internal structure of the nucleus which facilitate the understanding of the properties of nucleons (neutrons and protons), the mechanisms of nuclear reactions (spontaneous or induced), in order to describe the different processes of elastic and inelastic nucleus-nucleus interactions, the fields of application of nuclear physics and, finally, the impact of nuclear radiation on human health and the environment.

In general, nuclear physics is the physics of low energies, ranging from 250 eV to 10 GeV [SAO 04, GER 07, LAL 11]. The range of energies above 10 GeV [SAO 04, GER 07, LAL 11] relate to the physics of high energies whose purpose is to study the constituent particles of matter and the fundamental interactions between them. In this field, experimenters use particle accelerators that operate at very high energies or deliver very large beam intensities, thus allowing access to the fundamental laws of subatomic physics at very short distances. The most spectacular achievement to date is of course the Large Hadron Collider (LHC), launched in September 2008 at CERN.

Nuclear physics is an area that has experienced considerable growth since the discovery of radioactivity in 1896 by Henri Becquerel [HAL 11], well before the discovery of the atomic nucleus in 1911 by Ernest Rutherford [RUT 11]. Research in nuclear physics covers several topics ranging from subatomic particles to stars. It thus constitutes a fundamental component of physics, allowing the exploration of the infinitely large and the infinitely small [ARN 10]. In addition, nuclear physics makes it possible to understand many astrophysical

phenomena such as nucleosynthesis processes (primordial, stellar and explosive) within the framework of the Big Bang model. The study of these processes allows us to understand the origin of chemical elements and to describe the evolution of supernova and neutron stars [SUR 98].

This book is the fruit of a 25-year long teaching career. Initially this was teaching final-year high-school S1 and S2 science students at Alpha Molo Baldé High School in Kolda, from 1996 to 2002. It was then at Bambey High School from 2002 to 2008 and at Maurice Delafosse Technical High School from 2008 to 2010. This was followed by 9 years at Assane Seck University, Ziguinchor, teaching final-year Physics undergraduates and, since February 2019, teaching final-year Physics and Chemistry undergraduates at the University of Thiès.

Nuclear Physics 1 consists of four chapters, as follows.

Chapter 1 is reserved for general information regarding the *atomic nucleus* with a view to establishing the general properties of nuclei. It begins with a presentation of the experimental facts that led to the *discovery of the electron* (β^- particle), the *proton*, the *neutron* and the *nucleus* itself. It then focuses on the study of the *composition* and *dimensions* of the nucleus. Next, the *nomenclature of nuclides* and the *stability of nuclei* are studied. The chapter culminates with a series of exercises with answers.

Chapter 2 is dedicated to the study of nuclear deexcitation processes. The *nuclear shell model*, which offers an understanding of the discrete structure of nuclear levels, is studied in detail. Subsequently, the study examines the properties of *angular momentum* and *parity*, the processes of *gamma deexcitation* and *internal conversion* and the phenomenon of deexcitation by nuclear emission. A detailed study of the Bethe-Weizsäcker *semi-empirical mass formula* via the liquid-drop model and of the *mass*

parabola equation for odd A completes the chapter and is followed by a series of exercises complete with answers.

Chapter 3 is devoted to the study of *alpha* (α) *radioactivity*. It begins with the experimental facts that led to the discovery of *radioactivity* itself, the discovery of α radioactivity and β^- radioactivity, the discovery of the *positron* (β^+ particle), *neutrino* and experiments highlighting α , β and γ *radiation*. The chapter goes on to focus on the study of *radioactive disintegration* and the properties of α *decay*. A series of exercises complete with answers is at the end of the chapter.

Chapter 4 is reserved for the study of β^- and β^+ *decay modes* and for the study of *radioactive family trees*. At the beginning of the chapter, we present the experimental facts that led to the discovery of *artificial radioactivity*. We then focus the development on the study of the properties of β *decay* and the link between β decay and decay by *electron capture*. In addition, *double β decay* and the process of *atomic deexcitation* by *Auger effect* are studied in this chapter. The study subsequently focuses on the presentation of *radioactive series*, enabling the introduction of the *Bateman equations*. The mechanism for *radionuclide production* by nuclear bombardment features prominently in the chapter, which is rounded off with a series of exercises complete with answers.

Two appendices follow the above chapters. The first appendix is dedicated to the determination of the quantified expression of the energy of the three-dimensional quantum harmonic oscillator, in relation to the harmonic potential nuclear shell model. Two approaches are adopted to achieve this. The first approach integrates the Schrödinger equation applied to a quantum harmonic oscillator. In the second approach, a more flexible operative approach is adopted using creation and annihilation

operators. The second appendix provides a listing, in table form, of the atomic masses of isotopes of atomic numbers $Z = 1-93$.

This book is written for Physical Science teachers in high schools, for final-year Physics undergraduate students (*Licence 3* under the French LMD system) and for university lecturers responsible for the Nuclear Physics module in their programs. It is written using clear and concise language, underpinned by a very original pedagogical style. Each chapter begins with an overview of the general objective, the specific objectives and the prerequisites for understanding the chapter as it unfolds. In addition, each concept or law introduced follows a direct application for sound understanding of the nuclear phenomena and properties studied. The chapters are interspersed with succinct biographies of all the great thinkers who have contributed to the development of nuclear physics in relation to the topics developed.

This book does not attempt to cover all aspects relating to understanding nuclear deexcitation processes and the properties of spontaneous nuclear reactions. Nevertheless, it contains the fundamental basics of nuclear physics relating to the topics studied here. As with all human endeavors, there is always room for improvement. We therefore remain open to our readers for any suggestions, comments or criticisms that could be used to improve the scientific quality of this work.

September 2021

1

Overview of the Nucleus

Overall objective	
To know the general properties of nuclei	
Specific objectives	
To compare the atomic models of Thomson, Perrin and Rutherford	To define the effective scattering cross-section
To compare Rutherford's and Blakett's observations on the first nuclear transmutation reaction	To define the effective elementary scattering cross-section
To know the properties of the isospin operator	To define the separation energy of a nucleon
To know the properties of the spin angular momentum of a nucleus	To determine the separation energy of a neutron from a proton for a given nuclide
To know the fundamental properties of nucleons	To determine the total isospin corresponding to the ground state of a nucleus
To know the expression for the radius of a nucleus assumed to be spherical	To deduce, from the binding energy, the nuclear charge of the most stable isobar
To know the expression for the Sakho unit nuclear radius	To establish the relationship between binding energy and mass defect
To know the principle of a mass spectrograph	To establish the relationship between skin thickness and the diffusivity parameter
To compare the stability of nuclei from their nuclear binding energy	To write the balanced equation of the first nuclear transmutation reaction
To know the effect of nuclear	To establish Rutherford's

forces on the stability of nuclei	differential effective cross-section
To differentiate between u and d quarks according to the Gell-Mann and Zweig model	To make the analogy between electron gyromagnetic ratio and nuclear gyromagnetic ratio
To differentiate between isospin and nuclear spin	To make the analogy between Bohr magneton and Bohr nuclear magneton
To differentiate between unit nuclear radius and electromagnetic unit radius	To make the analogy between spin multiplicity and isospin multiplicity
To differentiate between isotopes, isobars and isotones	To interpret Chadwick's experiment
To differentiate between mirror nucleus and magic nucleus	To interpret Geiger and Marsden's experiment
To distinguish between valley of stability and line of stability	To interpret Rutherford's scattering experiment
To define a monoisotopic element	To interpret Rutherford's nuclear transmutation experiment
To define a nuclear isomer	To interpret the shape of the Woods-Saxon charge distribution density
To define the nuclear dipole magnetic moment	To interpret the Segrè diagram
To define the nuclear Landé factor	To interpret the Aston curve
To define the skin thickness of a nucleus	To situate the nuclear energy surface or stability

	valley in the Segrè diagram
To define the atomic mass unit	
Prerequisites	
Material structure	Motion of a charged particle in a uniform magnetic field
Atomic models	Vector product properties
Shell model of electron configurations	Fundamental theorems of the dynamics of the material point
Quantum numbers of the electron	

1.1. Discovery of the electron

1.1.1. *Hittorf and Crookes experiments*

In around 1869, Johann Wilhelm Hittorf studied electric discharge in rarefied gases using a vacuum tube. With the help of a Sprengel pump, Hittorf managed to obtain pressures below 0.001 mbar and found that electric discharges were accompanied by the emission of glow rays, which he called “cathode rays” [LEP 56, CAR 79, ROU 60, PER 95, SAK 11]. Subsequently, he observed that cathode rays are gifted with the property of being deflected by a magnetic field. But Hittorf stopped at these observations, without providing any physical interpretation.

Still in 1869, Sir William Crookes invented the electronic tube bearing his name [CRO 79, ROU 60, SAK 11]. The *Crookes tube* was a cold cathode tube, that is, a tube that did not have a heating filament as in the case of cathode tubes, designed to generate electrons.

Essentially, a Crookes tube is a bulb containing a gas and is equipped with two electrodes ([Figure 1.1](#)). When a voltage of approximately 50,000 volts is applied between the two electrodes and the gas pressure is gradually reduced, a dark space (called Crookes space) fills the tube at around 0.01 millimeters of mercury. Today it is now possible to interpret Crookes' observations.

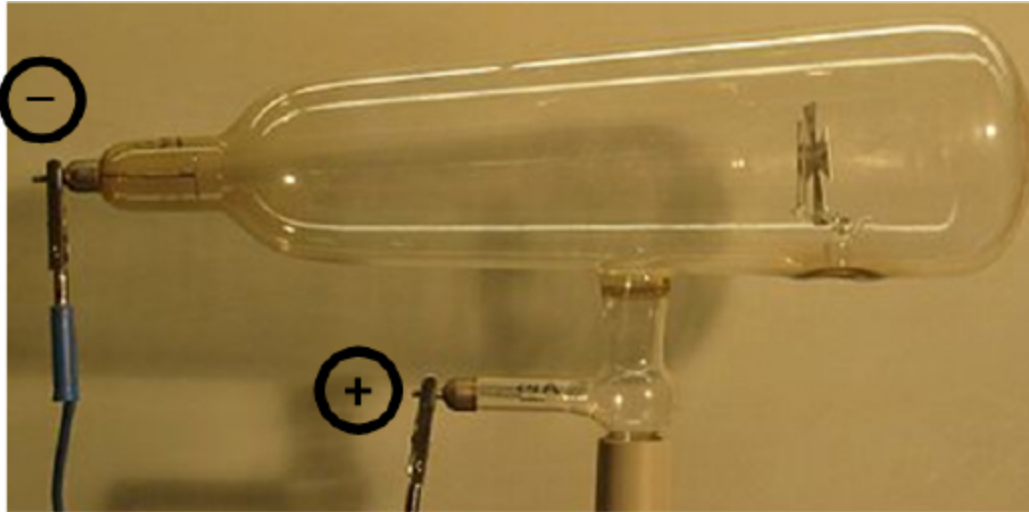


[Figure 1.1.](#) *Crookes tube*

Inside the Crookes tube, electrons are generated by ionization of gas molecules excited by the applied continuous voltage. Under the action of the established electric field, the ions created in the tube are accelerated. They collide with gas molecules, knocking electrons off them. The positive ions thus formed are attracted by the cathode. As they strike the latter, they eject a large number of electrons, called cathode rays. As they strike the glass, the electrons excite the atoms in the walls of the tube, thus causing its fluorescence usually in the yellow-green range. The electrons flow in a straight line from the cathode to the anode. This motion is highlighted by the shadow cast by the cross on the fluorescent wall ([Figure 1.2](#)). Moreover, cathode radiation has the property of being deflected by a magnetic field. Crookes considered cathode radiation to be

the fourth state of matter which he called the radiant state. But what is the nature of this radiation?

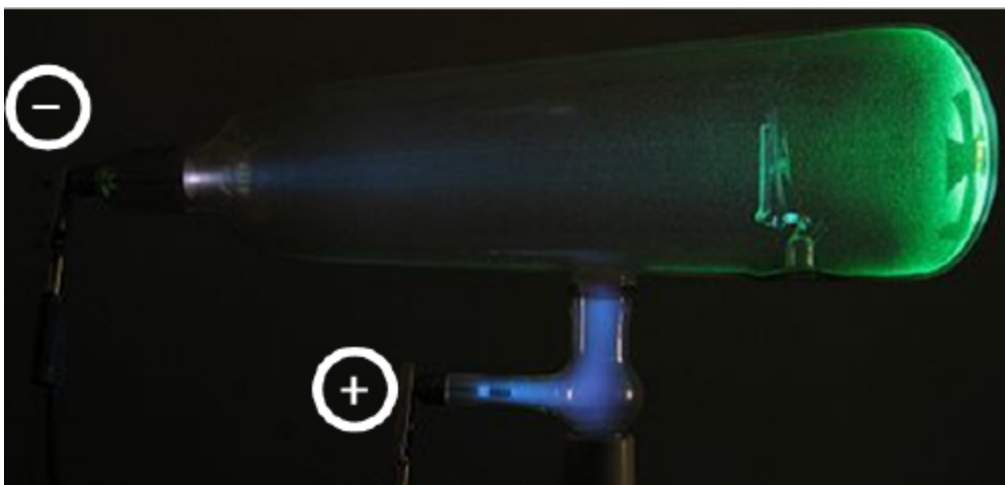


Figure 1.2. *Crookes tube wall fluorescence*

Crookes gave the following response to this question in 1885: “cathode radiation consists of negatively charged molecules emitted by the negative electrode”. The proof that they are indeed molecules, he cried, is that the action of a magnet makes them deviate from their trajectory, just like particles of iron filings.

Box 1.1. Hittorf (1824-1914); Crookes (1832-1919)

Johann Wilhelm Hittorf was a German physicist. He is also known for his work on the interpretation of electrical conductivity in electrolytic solutions in 1859, on the quantitative study of metal ion allotropy in 1865 and on the demonstration of cathode rays in 1869.

Sir William Crookes was a British physicist and chemist. He is most famous for having invented the “Crookes tube” in 1869 which allowed him to highlight cathode rays.

1.1.2. Perrin and Thomson experiments

While cathode radiation was an experimental reality that no-one could question, the molecular nature of the famous radiation puzzled many physicists, including Sir Joseph John Thomson [THO 97, ROU 60, CAR 79, PER 95, FAL 87, SAK 11]. The latter, as early as 1881, boldly took the opposite view to Crookes' conception of the nature of cathode radiation. For Thomson, "cathode radiation consists not of molecules but of *particles of pure negative electricity*," which he would later call electrons (a term introduced in 1891 by Stoney [CAR 79]). However, Thomson argued that "particles of pure electricity are not matter". Moreover, he noted, even if experimental observations require particles of pure electricity to be given a mass, then it is only necessary to understand that "this mass is nothing other than their inertia induced by their motion under the action of the magnetic field". However, Thomson did not say anything regarding the dimension of particles of pure negative electricity.

Challenging the ideas of Crookes, Thomson and others, Perrin suggested that cathode rays should not be considered as being made up of molecules but of "smaller particles charged with pure negative electricity". In 1895, he sought to verify this proposal through experimentation. Perrin then used a Faraday box (a small cylinder capable of trapping cathode rays), in contact with the plate of a positively-charged electroscope ([Figure 1.3](#)), to gather the cathode radiation as it exited a Crookes tube.

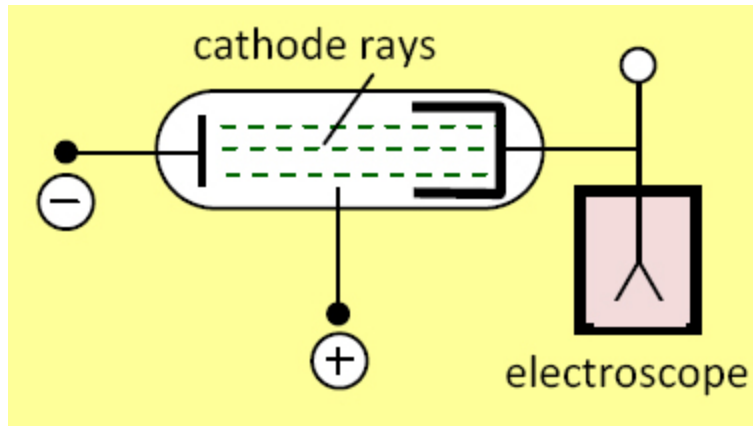


Figure 1.3. *Perrin's simplified experimental set-up*

Perrin found that the famous particles of pure electricity suggested by Thomson roughly neutralized the positive charge of the electroscope. These observations confirmed that the electricity transported by cathode radiation is negative in nature. But it should be noted that, until that date, there was no information on the size of the particles of pure negative electricity. Were they smaller than atoms? This question could be answered by measuring their mass, m . In chronological terms, the measurement of this mass was preceded by the measurement of the electron mass-to-charge ratio, e/m , by Thomson, and by the measurement of the elementary electrical charge, e , by Robert Millikan. Thomson's experiments form the subject of the study that follows. Millikan's experiment is discussed in [section 1.1.3](#).

In 1897, Thomson conducted a series of historical experiments that measured the mass-to-charge ratio of the electron.

First experiment: Thomson studied the possibility of separating the negative electrical charge from the cathode rays by a magnetic field. He built a cathode-ray tube that ends in a pair of cylinders with slots connected to an electrometer. This first experiment showed that the cathode rays are not deflected under the action of a magnetic field. Thomson concluded that the negative charge cannot be

separated from the rays (which tacitly proves that the cathode rays are composed of identical charges).

Second experiment: Thomson studied the action of an electric field on cathode rays. To do this, he built a cathode-ray tube with a deeper vacuum, within which is an electric field created by a voltage applied between two conductive metal plates. He placed a coat of phosphorescent paint at the end of the tube to detect incident rays. Thomson observed that rays are attracted by the positive plate. He thus proved that the electrical charge of cathode rays is negative, in accordance with Perrin's experimental observations.

Third experiment: Thomson sought to measure the *electron mass-to-charge ratio*, e/m . Today, Thomson's experiment is replicated by performing more meticulous experiments to determine the value of e/m .

Electrons in a constant velocity beam penetrate at O into a space where uniform electric and magnetic fields can occur simultaneously. In a first experiment, the orthogonal electric and magnetic fields are applied simultaneously so that the motion of the electrons is straight and uniform along OO' ([Figure 1.4\(a\)](#)). The electric field is vertical and directed downwards. In a second experiment, the magnetic field is removed; the characteristics of the electric field and the electron velocity vector remain unchanged ([Figure 1.4\(b\)](#)). The set-ups of the two experiments conducted can be schematically presented in parallel, as shown in [Figure 1.4](#).

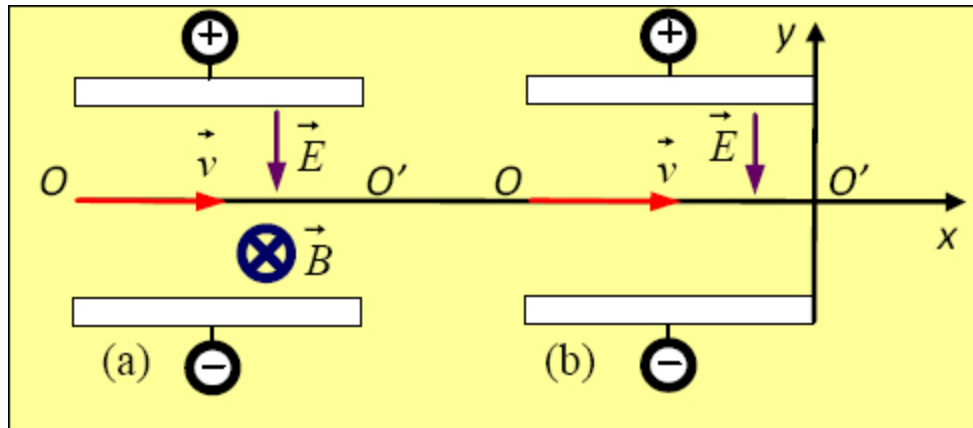


Figure 1.4. *Simplified set-up for measuring the electron mass-to-charge ratio: (a) simultaneous action of the electric field and the magnetic field; (b) action of the electric field alone*

It is then shown that the electron mass-to-charge ratio has the following value:

$$\frac{e}{m} = 1.76 \times 10^{11} \text{ C} \cdot \text{kg}^{-1} \quad [1.1]$$

APPLICATION 1.1.- Using the device shown in [Figure 1.4](#), show that if Y designates the vertical deviation along the $O'y$ axis, the electron mass-to-charge ratio is given by the expression:

$$\frac{e}{m} = 2 \frac{E}{B^2 l^2} Y \quad [1.2]$$

Then find the result [\[1.1\]](#).

Given data: $E = 50 \text{ kV} \cdot \text{m}^{-1}$; $B = 1 \text{ mT}$; $OO' = l = 10.0 \text{ cm}$, $Y = 1.76 \text{ cm}$.

ANSWER.- Considering [Figure 1.4\(a\)](#), the electrical force is compensated by the magnetic force since the motion is uniform and rectilinear (it is a velocity filter). Let:

$$q\vec{E} = -q\vec{v} \wedge \vec{B} \Rightarrow v = \frac{E}{B} \quad [1.3]$$

Let us thus determine the equation of the trajectory of an electron in the electric field ([Figure 1.4\(b\)](#)). Using the theorem of the center of inertia gives:

$$\begin{cases} q\vec{E} = m\vec{a} \\ \vec{a} = \frac{q\vec{E}}{m} \end{cases} \Rightarrow \begin{cases} a_x = 0 \Rightarrow x = vt \\ a_y = -\frac{qE}{m} \Rightarrow y = -\frac{1}{2} \frac{qE}{m} t^2 \end{cases}$$

Using the last equation system, the equation for the trajectory of an electron within the electric field is written ($q = -e$):

$$y = \frac{1}{2} \frac{eE}{mv^2} x^2 \quad [1.4]$$

The vertical deviation, Y , along the $O'y$ axis is obtained for $x = OO' = l$. Using [\[1.4\]](#) and taking account of [\[1.3\]](#), we then obtain the following:

$$Y = \frac{e}{m} \frac{B^2}{2E} l^2 \quad [1.5]$$

Using [\[1.5\]](#), result [\[1.2\]](#) is found.

NOTE.-

$$\frac{e}{m} = 2 \frac{5 \times 10^4}{10^{-6} \times 10^{-2}} \times 1.76 \times 10^{-2} = 1.76 \times 10^{11} \text{ C} \cdot \text{kg}^{-1}$$

The result [\[1.1\]](#) is indeed found.

The CODATA (Committee on Data and Technology) recommended value is $1.75882001076(53) \times 10^{11} \text{ C} \cdot \text{kg}^{-1}$.